Electrodeposition of Metal Nanostructures by Galvanic Displacement Powered with Insoluble Crystals of a Ferrocene Derivative

Robert A. W. Dryfe,*[a] Erich C. Walter,[b] and Reginald M. Penner*[b]

The deposition of metal nanostructures (wires and particles) on a graphite surface from an aqueous electrolyte solution was induced by galvanic displacement, via the oxidation of insoluble crystals of a ferrocene derivative (either n*-butyl ferrocene or decamethyl ferrocene) present on the same substrate. Micron-to-millimetre-scale crystallites of decamethyl ferrocene were deposited on the graphite surface by evaporation from a solution of a nonpolar solvent (1,2-dichloroethane). Immersion of this modified surface into a dilute solution of a metal ion (e.g., Cu^{II}, Ag^{I}, Pd^{II}, Pt^{II} and others) caused the deposition of metal nanoparticles at step edges present on the graphite surface. The reducing equivalents required for the metal deposition process are provided by oxidation of the ferrocene derivative on the surface, as directly evidenced by elemental analysis and chronoamperometric experimental data presented here.*

Introduction

Tremendous effort is being expended to develop new methods for preparing nanoparticles and nanowires composed (principally) of metals and semiconductors.[1] Solution phase methods of metal deposition have shown promise with regard to nanostructure fabrication.[2] Amongst these, electrochemical methods have been presented as viable, controllable routes to the preparation of nanowires and nanoparticles.[3] Electrochemical methods are attractive because control of the electrode potential permits the rate and temporal profile of nanostructure growth to be controlled with precision.

Herein, we describe the preparation by spontaneous (galvanic) displacement of metal nanostructures on highly oriented pyrolytic graphite (HOPG) surfaces. Two aspects of the reported results are novel: i) the galvanic displacement of nanostructures was powered by the concurrent oxidation of *insoluble* layers of ferrocene derivatives. The organic material was predeposited onto the graphite surface prior to immersion in the aqueous metal-plating bath; ii) the method described here "automatically" produced metal nanostructures, without external intervention to control the growth potential or growth time.

The experiment described here constitutes an extension of the seminal prior work of Bond et al.,[4–7] Scholz et al.[8–10] and others,[11–13] who have explored the solid-state electrochemistry of insoluble crystalline overlayers in great detail. This prior literature has demonstrated that the solid-state oxidation (or reduction) is accompanied by the uptake of an anion (or cation) from the contacting aqueous electrolyte at the three-phase boundary.[4,9,10] The observed voltammetric responses are well-defined, and the energetics and kinetics of electron transfer at these organic crystals depend not only on the identity of the organic compound, but also on the identity and concentration of the electrolyte present.

Other studies of relevance span work, where hydrophobic electrode surfaces–-normally of basal plane graphite—were modified with microdroplets of redox-active oils and immersed in aqueous electrolytes, have also been reported.[14–16] Hydrophobic aromatic amines and ferrocene derivatives figure amongst the molecules studied using this approach.[15,17,18] The hydrophobic molecules deposited on the electrode surfaces can be present as pure liquids or in solutions of appropriate organic solvents.[17] In the latter case, since the electron-transfer process is coupled to interfacial ion transfer, the voltammetric response can be used to determine the energetics of ion transfer across immiscible liquid phases.[19,20] An alternative approach uses a continuous thin film of the organic phase on the electrode surface, rather than a dispersion of microdroplets, to probe charge-transfer processes at liquid/liquid (L/L) interfaces.[21,22] This immiscible-liquid work provides a bridge to L/L electrochemistry, where interfacial charge transfer was studied via direct polarisation of the L/L interface using four-electrode systems or, indirectly, using the scanning electrochemical microscope.[23]

Recently, a number of reports have described the deposition and/or spontaneous assembly of metallic nanoparticles at L/L interfaces.[24–27] These processes generally consist of the reduction of an aqueous-phase metallic precursor by an organic-phase electron donor. Both spontaneous and electrochemically driven deposition processes have been reported.[24,25,28,29] Furthermore, Compton and co-workers have added silver(I) ions

[a] *Dr. R. A. W. Dryfe*
Department of Chemistry, University of Manchester
Institute of Science & Technology, PO Box 88,
Manchester M60 1QD (UK)
Fax: (+44) 161-200-4559
E-mail: robert.dryfe@umist.ac.uk

[b] *E. C. Walter, Prof. R. M. Penner*
Department of Chemistry, University of California
Irvine, California 92679-2025 (USA)
Fax: (+1) 949-824-3168
E-mail: rmpenner@uci.edu

 DOI: 10.1002/cphc.200400298

to their aqueous electrolyte in the aforementioned microdroplet experiments: spontaneous silver deposition at the microdroplet boundaries provided further evidence to support the electrolysis mechanism of the microdroplets, although no detailed study of the morphology or conditions of formation of the metals has been reported to date.[18]

Herein, we report that overlayers of two ferrocene derivatives, when deposited on HOPG surfaces, are capable of driving the electrochemical deposition of metal nanoparticles and nanowires. We propose that the mechanism responsible for this metal deposition, shown in Scheme 1, is a galvanic displacement driven by the coupled oxidation of these organic crystals. Attention is focused in this paper on the nature of the metal deposit and on the mechanism of the deposition reaction. Scanning electron microscopy (SEM) was used to monitor the distribution both of organic crystallites and the deposited metal on the graphite surface. Electrochemical measurements coupled with energy-dispersive X-ray analysis (EDX) were used to verify the mechanism of the deposition process. We believe the mechanism is generic and deposition could, therefore, be extended to other water-insoluble electron donors, such as the hydrophobic amine derivatives referred to above or hydrophobic quinone species. Ferrocene derivatives were chosen in this case mainly because of the considerable prior literature on the modification of graphite electrode surfaces with this class of electron donor (see below).

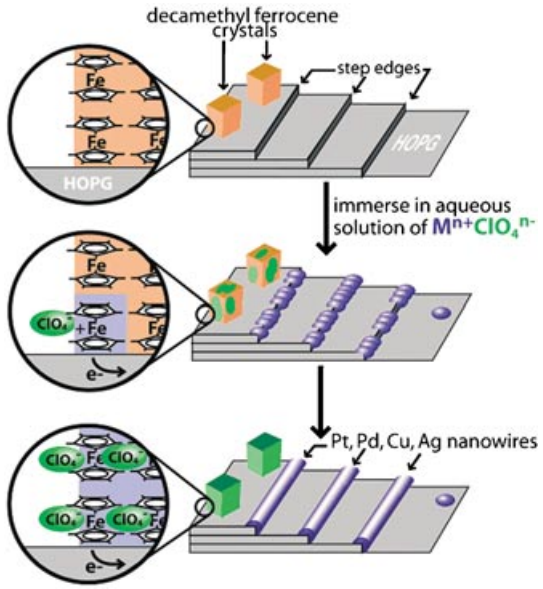

Scheme 1. *Proposed mechanism for the spontaneous electrodeposition of metal and the concurrent incorporation of anions into the surface of decamethyl ferrocene crystals as these become oxidised. Electrons from the ferrocene derivative are coupled through the graphite substrate to defects at which the reduction of metal ions from solution occurs. Charge compensation occurs through the contacting electrolyte phase.*

Results and Discussion

Preparation and Characterisation of $(CH_3)_{10}$–Fc and *n*Bu–Fc Modified HOPG Electrodes

The modification of graphite electrode surfaces with both *n*Bu–Fc and $(CH_3)_{10}$–Fc has previously been reported,[6,15] with $(CH_3)_{10}$–Fc, in particular, being described as an "ideal" system for the voltammetric study of electrodes covered with such insulating materials.[4] $(CH_3)_{10}$–Fc and *n*Bu–Fc were deposited on HOPG surfaces by evaporation of 1–10 μL of solutions in 1,2-dichloroethane (DCE) with a concentration in the range from 1–10 mM to produce a mean coverage in the range from 10^{-9}–10^{-7} moles cm^{-2} on the about 1.0 cm^2 HOPG surface. Because it is a solid at room temperature, SEM images of $(CH_3)_{10}$–Fc-covered surfaces can be obtained, and typical images are shown in Figure 1. It is apparent that the $(CH_3)_{10}$–Fc is highly dispersed on the HOPG surface and is present both as microcrystallites, which seem to align with the direction of step edges (Figure 1a), and as a thin porous layer (visible in Figure 1b), which blankets the basal plane regions of the surface. Surfaces such as these served as the starting point for the galvanic displacement experiments involving $(CH_3)_{10}$–Fc, which will be described next. It was not possible to image *n*Bu–Fc-covered HOPG surfaces by SEM because of this material's liquid nature at room temperature, but its behaviour in the experiments to be described next was similar to that of $(CH_3)_{10}$–Fc.

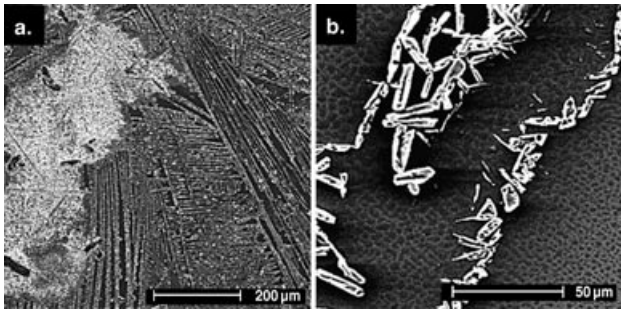

Figure 1. *a) Low- and b) high-magnification SEM images of an HOPG surface after the deposition of 5 μL of 1.0 mM $(CH_3)_{10}$–Fc in DCE.*

Characterisation of Modified Surfaces after Contact with Metal-Plating Solutions

Contact of $(CH_3)_{10}$–Fc-modified graphite with aqueous solutions of palladium(II) complexes led to the spontaneous deposition of metallic Pd, consistent with recent reports at the L/L interface.[29] Figures 2a and 2b show the morphology of the Pd deposits on graphite, as revealed via SEM. As shown here, Pd preferentially deposited on step edges present on the HOPG surface and, in some places, this resulted in the formation of continuous wires with widths as narrow as 200 nm. In fact, the selectivity of nucleation for step edges was higher than that observed in prior attempts to grow palladium nanowires potentiostatically on HOPG.[3,30]

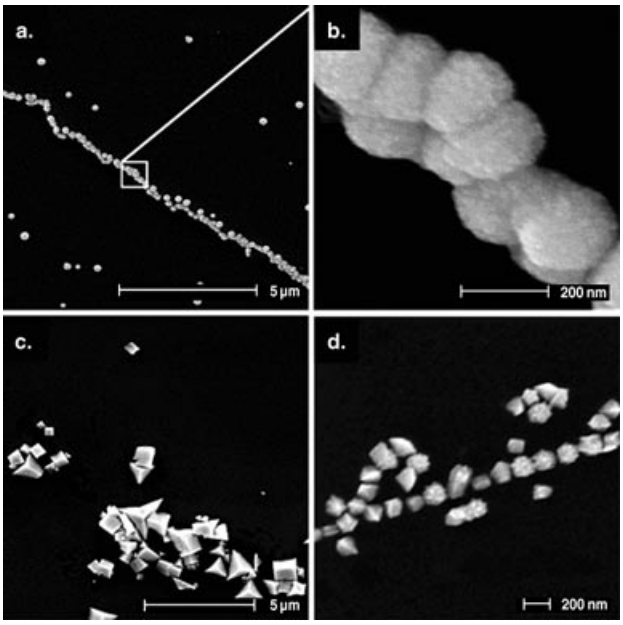

Figure 2. *a) Low- and b) high-magnification SEM images of Pd deposits formed by spontaneous reduction with dried $(CH_3)_{10}$–Fc. 10 μL of a 10 mM solution in DCE were deposited on the graphite surface and, once the DCE had evaporated, left in contact with a 1.0 mM aqueous solution of $(NH_3)_2Cl_4Pd$, which also contained 0.1 M lithium chloride and 1 M lithium perchlorate. c) Low- and d) high-magnification SEM images of Cu deposits formed in an analogous manner to the palladium deposit, except that a 1.0 mM solution of cupric sulfate was used as the metal precursor.*

The deposition of Pd was only observed to occur when the metal-plating solution was in contact with regions of the HOPG on which $(CH_3)_{10}$–Fc had been deposited. The metallic deposits adhered strongly to the graphite surface insofar as they persisted on the surface after rinsing with water (to remove excess electrolyte) and were not visibly affected by the electron beam of the SEM. Metal deposition did not occur if the organic solvent had not fully evaporated at the time when the aqueous electrolyte was added, since the organic solvent tended to wet the graphite surface, preventing contact between the aqueous phase and the graphite. Deposition was also not observed to occur on insulating substrates, such as freshly cleaved mica. Collectively, these observations are consistent with the mechanism of deposition shown in Scheme 1, as they suggest that both electronic and ionic conduction paths must be maintained between the electron donor and the metal precursor, with a counterflow of electrolyte ions balancing the reduction to the metal.

Figures 2c and 2d show deposits of copper, again formed in the presence of $(CH_3)_{10}$–Fc on the HOPG surface. Again, as shown in Figure 2d, the nucleation of copper occurred with a preference for step edges. Other metals, including Pt, Ag and Au, formed similar deposits. The metals were deposited from aqueous solutions of platinum(II), silver(I) and gold(III) using both *n*–Bu–Fc and $(CH_3)_{10}$–Fc as electron donors. Copper deposition was induced only where $(CH_3)_{10}$–Fc was employed as the electron donor, and the origin of this "selective deposition" is readily apparent from the cell potentials calculated in Table 1.[31,32] No evidence of deposition of Cd, Ni, Pb or MoO_2 was obtained when deposition was attempted from aqueous solutions of cadmium(II), nickel(II), lead(II) or molybdate, using either $(CH_3)_{10}$–Fc or *n*Bu–Fc and, again as shown in Table 1, the deposition of these materials is thermodynamically unfavourable. EDX was used to confirm the identity of the metallic deposits, with the copper deposits in particular showing evidence of oxide formation.

Investigations of the Mechanism for Spontaneous Metal Electrodeposition

Further evidence in support of the mechanism of Scheme 1 was obtained by probing the elemental composition of the organic layer using EDX after the spontaneous deposition of palladium onto the same surface. All four spectra shown in Figure 3 exhibit the *K*-shell signals for Fe associated with the $(CH_3)_{10}$–Fc layer at approximately the same intensity. In the experiments of Figures 3a and 3b palladium deposition was carried out in electrolytes containing iodide and perchlorate ions, respectively, and the presence of these ions is seen in the EDX spectra of the organic layer even after rinsing with water. Note also that *L*-shell signals for Pd are seen in both of these spectra. ClO_4^- and I^- were not incorporated into the organic layer in the absence of palladium in the contacting electrolyte (Figures 3c and 3d). We conclude that oxidation of the organic deposit by the solution-phase metal ion leads to the uptake of the electrolyte counterion in the deposit, as has been reported for electrochemical studies of such insoluble deposits.[4] These EDX data provide direct evidence for the oxidation of the organic layer concurrent with the deposition of metallic palladium.

Another test of the hypothesis embodied by Scheme 1 involves carrying out the two reactions—metal ion reduction and oxidation of the ferrocene deriva-

Table 1. *Standard reduction potentials for deposition reactions and approximate cell potentials versus $(CH_3)_{10}$–Fc and* n*Bu-Fc.*

Deposition Reaction	E^0 [V vs. NHE][a]	E_{cell} [V vs. $(CH_3)_{10}$–Fc][b]	E_{cell} [V vs. *n*Bu-Fc][a]
$MoO_4^{2-} + 2H_2O + 2e^- \rightarrow MoO_2 + 4OH^-$	−0.96	−1.03	−1.52
$Cd^{2+} + 2e^- \rightarrow Cd^0$	−0.40	−0.47	−0.96
$Ni^{2+} + 2e^- \rightarrow Ni^0$	−0.257	−0.327	−0.817
$Pb^{2+} + 2e^- \rightarrow Pb^0$	−0.125	−0.132	−0.685
$Cu^{2+} + 2e^- \rightarrow Cu^0$	+0.340	+0.270	−0.220
$PdCl_4^{2-} + 2e^- \rightarrow Pd^0 + 4Cl^-$	+0.64	+0.57	+0.08
$PtCl_4^{2-} + 2e^- \rightarrow Pt^0 + 4Cl^-$	+0.76	+0.69	+0.20
$Ag^+ + e^- \rightarrow Ag^0$	+0.80	+0.73	+0.24
$AuCl_4^- + 3e^- \rightarrow Au^0 + 4Cl^-$	+1.0	+0.93	+0.44

[a] See ref. [31] a–c. [b] These cell potentials were calculated using E^0 values for $(CH_3)_{10}$–Fc and *n*Bu-Fc in DCE of +0.07 V and +0.56 V versus NHE, respectively, see ref. [32].

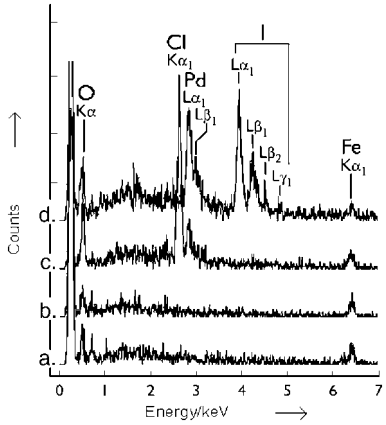

Figure 3. *EDX analysis of $(CH_3)_{10}$–Fc-modified surfaces (10 μL of a 10 mM solution in DCE) after the exposure of these surfaces for 2 minutes to the following solutions: a) 1.0 mM $(NH_3)_2Cl_4Pd$ in aqueous 0.10 M KI, b) 1.0 mM $(NH_3)_2Cl_4Pd$ in 0.10 M $LiClO_4$, c) aqueous 0.10 M KI, d) aqueous 0.10 M $LiClO_4$.*

tive—on different pieces of graphite. This was accomplished by using a two-compartment cell in which two graphite electrodes, connected by a copper wire, were immersed in separate half-cells, which contained different aqueous electrolytes. These cells were ionically shorted via a salt bridge, as shown schematically in Figure 4 A. This approach permitted the transient current for the spontaneous reduction to the metal to be directly recorded, which allowed a comparison to be made between various reactive metals. Nine different metals and one metal oxide (Table 1) were evaluated using this apparatus.

The quantity of deposited $(CH_3)_{10}$–Fc exerted a strong effect both on the rate of metal deposition and on the quantity of deposited metal. The effect of the quantity of deposited $(CH_3)_{10}$–Fc is examined for the deposition of palladium, for example, in Figure 4 B. The level of reproducibility of the response may be gauged by comparing curves (a) and (b) for which the quantities of $(CH_3)_{10}$–Fc were identical. The transient current, and therefore the quantity of deposited metal, was limited, in part, by the volume of organic material deposited on the electrode, as the comparison of series (c) with series (a) demonstrates. The current in series (c) approaches that of the background response, series (d), once approximately 10 μC of charge have passed [which corresponds to ca. 25% of the $(CH_3)_{10}$–Fc deposit]. This observation is consistent with previous voltammetric studies of immobilised $(CH_3)_{10}$–Fc, which have indicated that substantial potentiostatically driven electrolysis of this material is possible when it is present in a microcrystalline form.[4,6] By contrast, when a greater volume of $(CH_3)_{10}$–Fc is deposited [as in series (a)], the transient current remains significantly above the background level throughout the period recorded. Comparison of the current responses of series (a) and (c) reveals that the transient currents are not, however, directly proportional to the volume of $(CH_3)_{10}$–Fc applied. The early portion of the transient response may be judged to be limited by the nucleation and growth of the metallic deposits, since a characteristic current "peak" is observed at about 15 seconds [series (a), ca. 6 seconds for series (c)]. These observations suggest that the current response passes

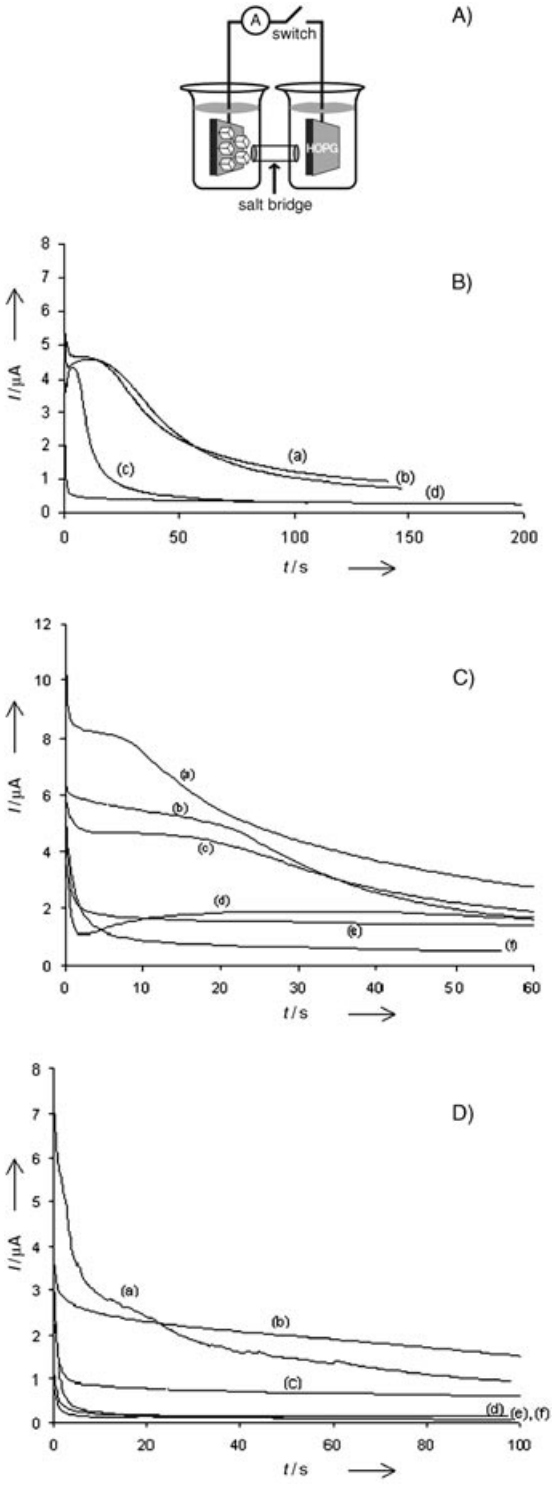

Figure 4. *Current transients obtained with the apparatus shown schematically in (A). B) The effect of the quantity of deposited $(CH_3)_{10}$–Fc on the deposition of palladium is probed. For all traces, the right-hand half-cell consisted of a bare HOPG surface immersed in aqueous 1 mM $(NH_3)_2Cl_4Pd$, 0.1 M LiCl, 1 M $LiClO_4$. The left-hand half-cell contained aqueous 1 M $LiClO_4$, and the coverage of $(CH_3)_{10}$–Fc on the HOPG in this compartment was varied as follows: (a) 5 μL, (b) 5 μL repeated, (c) 2 μL, (d) 0 μL. C) and D) Deposition transients for different metals versus 5 μL of a 2 mM DCE solution of $(CH_3)_{10}$–Fc (C) and nBu-Fc (D). The following metal salts were present along with 1 M lithium perchlorate in the portion of the cell not containing $(CH_3)_{10}$–Fc: (a) 0.2 mM $AuCl_3$, (b) 1 mM $AgNO_3$, (c) 1 mM $(NH_4)_2PdCl_4$, (d) 1 mM $(NH_4)_2PtCl_4$ and, (e) 1 mM $CuSO_4$. Series (f) contained no metal ions and thus served as a "background".*

from an initial limitation, caused by the rate of metal deposition, to a subsequent limitation, due to the organic deposit, as the extent of oxidation of this deposit increases. The background current response, series (d), was obtained where the Pd precursor was absent from the cell: identical responses were obtained in the presence of Pd when no $(CH_3)_{10}$–Fc was present in the cell.

The effectiveness of $(CH_3)_{10}$–Fc and *n*Bu–Fc crystals in driving the metal deposition process was probed for eight further metals and a metal oxide (MoO_2) using the two-compartment cell depicted in Figure 4A. The transient responses obtained with gold(III), silver(I), palladium(II), platinum(II), copper(II) and a background, which contained only the lithium perchlorate supporting electrolyte, are shown in Figure 4C. Responses that were essentially indistinguishable from the background response were obtained with nickel(II), lead(II), cadmium(II), protons and molybdate ions. Based on the arguments given earlier, gold deposition proceeds at the fastest initial rate and shows a more marked decrease as electrolysis proceeds, possibly as a consequence of concentration polarisation. The initial response (first 30 seconds) suggests that the trend in reactivity is: Au > Ag ≈ Pd > Pt ≈ Cu. The trend in E^0 values for the precursor ions of these metals is: Au > Ag ≈ Pt > Pd > Cu.[31] The observation that Pt is the only metal that does not follow the deposition trend predicted on the basis of the reduction potential may be related to the high surface energy of Pt, relative to Pd, which has recently been shown to affect its electrodeposition on well-defined metal-single-crystal electrodes and at the L/L interface.[33,34] The E^0 values quoted for all the reactive metals are positive of the value for $(CH_3)_{10}$–Fc in DCE [0.07 V vs. the normal hydrogen electrode (NHE)],[32] whereas the values versus NHE for the unreactive redox couples are −0.96 V (MoO_4^{2-}), −0.40 V (Cd^{II}), −0.26 V (Ni^{II}), −0.125 V (Pb^{II}) and 0.0 V (protons).[31]

Figure 4D depicts the transient response obtained using BuFc as the electron donor, rather than $(CH_3)_{10}$–Fc, for the solutions of Figure 4C. Essentially, an identical trend in reactivity is seen, except that the Cu^{II} solutions do not produce any measurable current relative to the background response. This observation is consistent with the E^0 value of Cu^{II}, which is lower than the value of 0.56 V vs NHE reported for *n*Bu–Fc in DCE.[32] Effectively, the general trends in reactivity with the two electron donors reflect the reduction potentials of metal compared to electron donor. The sole exception to this trend is again platinum, as explained above. The data for the various reactive metals with $(CH_3)_{10}$–Fc is summarised in Figure 5. The charge passed after 30 s is displayed as a function of the cell potential, that is, the difference in E^0 between the metal precursor and the electron donor. A general increase in charge passed with increasing cell potential is noted, with Pt being the only outlying point.

The behaviour observed also correlates with L/L experiments, where spontaneous deposition of Au, Ag, Pd, Pt and Cu can be induced at the water/DCE interface. Spontaneous deposition of Pd at this interface by organic phase $(CH_3)_{10}$–Fc has been reported recently, using a perchlorate common ion to preserve the electroneutrality of the aqueous and organic phases.[29] The deposition processes observed using solid-state $(CH_3)_{10}$–Fc as an electron donor were mirrored in the reactivity trends seen for the organic-phase electron donor: using the same aqueous-phase precursor salts; in addition to Pd, the deposition of Au, Ag, Pt and Cu was also observed at the L/L interface.

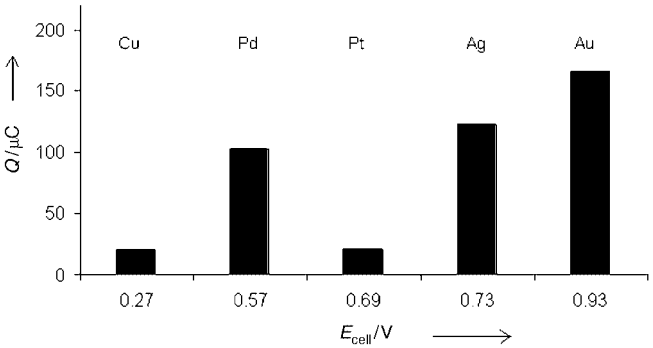

Figure 5. *Summary of reactivity information for the metals deposited using $(CH_3)_{10}$–Fc. The charge passed, Q, after an arbitrarily chosen time (30 s) is illustrated as a function of the cell potential, E_{cell}. The coulometric data is obtained from integration of the current transients of Figure 4c, following subtraction of the background transient [trace (f)].*

Conclusions

The spontaneous oxidation of insoluble layers of two ferrocene derivatives by dissolved aqueous-phase metal precursors was investigated. For metal precursors that react spontaneously, the products are nanoparticles and nanowires of the corresponding metals on the graphite surface. The method presented here relies on intrinsic surface defects (step edges) to create the structures deposited; the resolution of the deposit features thus tends to be limited by the width of the steps, in the first instance, and the amount of insoluble electron donor used to drive the deposition. Feature widths as low as 200 nm were observed in this study using spontaneous reduction on edges, although further improvement in the resolution may be possible. Nanostructures can also be deposited on solid surfaces by using the microcontact printing and dip-pen lithography approaches; feature sizes in the submicron regime have been reported using these techniques.[35,36] The intrinsic advantage of the step-edge approach is its simplicity, whereas the dip-pen and microcontact approaches offer enhanced control over the deposit structure.

A practical application for organic reducing agents, such as the ferrocenes investigated here, could be for anodically protecting nanometer-scale noble metal circuitry from corrosion. In this case, the organic crystals would perform the same function as the sacrificial zinc anodes commonly used for anodic protection of buried iron pipe and bridge abutments from corrosion. We also note that higher levels of organisation could be imparted to the metallic deposits by pretreatment of the conducting substrate to form hydrophilic and hydrophobic patterns on the surface.[37] The patterned surface could therefore be used to localise the aqueous and organic solutions,

and hence, impart further control to the deposit morphology over that imposed by the substrate step edges. Other techniques, which impose order on a deposit, such as the aforementioned dip-pen lithography and microcontact printing, could also be combined with the galvanic-displacement approach presented herein to generate more complex, hierarchical structures.

Experimental Section

Crystals of the ferrocene derivative were deposited on a 0.8 cm × 0.8 cm freshly cleaved highly oriented pyrolytic graphite surface (GE Advanced Ceramics Inc.) by evaporation of 1–10 μL of a dilute (1–5 mM) 1,2-dichloroethane (DCE, "spectro" grade, Acros Organics) solution. Two ferrocene derivatives were evaluated: bis(pentamethylcyclopentadienyl)iron [$(CH_3)_{10}$—Fc] and *n*-butylferrocene (*n*Bu-Fc), supplied by Acros Organics (Morris Plains, NJ, USA) and Alfa Aesar (Ward Hill, MA, USA), respectively. Note that $(CH_3)_{10}$—Fc recrystallizes from the organic solvent as microcrystals, whereas *n*Bu-Fc is a liquid at room temperature.

The metal salts employed were gold trichloride, silver nitrate, ammonium tetrachloroplatinate, ammonium tetrachloropalladate (all supplied by Alfa Aesar), cupric sulfate (Fisher), lead(II) nitrate, sodium molybdate, cadmium chloride, nickel(II) sulfate (all supplied by Aldrich). The salts were prepared as millimolar solutions in "Nano-pure" water (Barnstead, Dubuque, IA, USA). Aqueous solutions of perchloric acid (Fisher) and lithium perchlorate (Acros) were used in certain experiments, while potassium iodide was used as an alternative aqueous-phase electrolyte (Aldrich). The metal deposition current in the double surface experiment was monitored via a pico-ammeter (Keithley 427), connected to a PC using the Labview software. The salt bridge was formed from "Vycor" tips and filled with a 1 M aqueous solution of lithium perchlorate. SEM was carried out on uncoated samples using a Philips FEG-30XL microscope equipped with EDAX elemental analysis capabilities.

Acknowledgments

RAWD thanks UMIST for the award of study leave. This work was funded at UCI by NSF grant CHE-0111557. The authors thank Dr. Art Moore, formerly of GE Advanced Ceramics Inc., for donating the graphite used in these investigations.

Keywords: electrochemistry · interfaces · modified electrodes · nanostructures · self-assembly

[1] a) B. A. Parviz, D. Ryan, G. M. Whitesides, *IEEE Trans. Adv. Packag.* **2003**, *26*, 233. b) C. Murray, C. Kagan, M. Bawendi, *Ann. Rev. Mat. Sci.* **2000**, *30*, 545.
[2] a) M. Brust, M. Walker, D. Bethell, D. J. Schiffrin, R. Whyman, *J. Chem. Soc. Chem. Commun.* **1994**, 801. b) C. R. Martin, *Science* **1994**, *266*, 1961.
[3] a) R. M. Penner, *Acc. Chem. Res.* **2000**, *33*, 78. b) F. Favier, E. C. Walter, M. P. Zach, T. Benter, R. M. Penner, *Science* **2001**, *293*, 2227. c) R. M. Penner, *J. Phys. Chem. B* **2002**, *106*, 3339.
[4] A. M. Bond, *Broadening Electrochemical Horizons*, Oxford University Press, Oxford, **2002**, Ch. 5.
[5] A. M. Bond, F. Scholz, *J. Phys. Chem.* **1991**, *95*, 7460.
[6] A. M. Bond, F. Marken, *J. Electroanal. Chem.* **1994**, *372*, 125.
[7] M. F. Suarez, F. Marken, R. G. Compton, A. M. Bond, W. J. Miao, C. L. Raston, *J. Phys. Chem. B* **1999**, *103*, 5637.
[8] F. Scholz, B. Meyer, *Chem. Soc. Rev.* **1994**, *23*, 341.
[9] M. Lovric, F. Scholz, *J. Solid State Electrochem.* **1997**, *1*, 108.
[10] U. Schroder, K. B. Oldham, J. C. Myland, P. J. Mahon, F. Scholz, *J. Solid State Electrochem.* **2000**, *4*, 314.
[11] F. Marken, W. M. Leslie, R. G. Compton, M. G. Moloney, E. Sanders, S. G. Davies, S. D. Bull, *J. Electroanal. Chem.* **1997**, *424*, 25.
[12] F. Marken, S. Cromie, V. McKee, *J. Solid State Electrochem.* **2003**, *7*, 141.
[13] S. Zamponi, M. Berrettoni, P. J. Kulesza, K. Miecznikowski, M. A. Malik, O. Makowski, R. Marassi, *Electrochim. Acta* **2003**, *48*, 4261.
[14] F. Marken, R. D. Webster, S. D. Bull, S. G. Davies, *J. Electroanal. Chem.* **1997**, *437*, 209.
[15] J. D. Wadhawan, R. G. Evans, R. G. Compton, *J. Electroanal. Chem.* **2002**, *533*, 71.
[16] J. C. Ball, F. Marken, F. L. Qiu, J. D. Wadhawan, A. N. Blythe, U. Schroder, R. G. Compton, S. D. Bull, S. G. Davies, *Electroanalysis* **2000**, *12*, 1017.
[17] U. Schröder, J. D. Wadhawan, R. G. Evans, R. G. Compton, B. Wood, D. J. Walton, R. R. France, F. Marken, P. C. B. Page, C. M. Hayman, *J. Phys. Chem. B* **2002**, *106*, 8697.
[18] J. D. Wadhawan, R. G. Evans, C. E. Banks, S. J. Wilkins, R. R. France, N. J. Oldham, A. J. Fairbanks, B. Wood, D. J. Walton, U. Schröder, R. G. Compton, *J. Phys. Chem. B* **2002**, *106*, 9619.
[19] F. Scholz, S. Komorsky-Lovric, M. Lovric, *Electrochem. Commun.* **2000**, *2*, 112.
[20] S. Komorsky-Lovric, M. Lovric, F. Scholz, *J. Electroanal. Chem.* **2001**, *508*.
[21] C. Shi, F. C. Anson, *Anal. Chem.* **1998**, *70*, 3114.
[22] C. Shi, F. C. Anson, *J. Phys. Chem. B* **2001**, *105*, 1047.
[23] a) H. H. J. Girault, D. J Schiffrin in *Electroanalytical Chemistry, Vol* 15 (Ed. A. J. Bard) Marcel Dekker, New York, **1989**, p 1. b) V. Maracek, Z. Samec, J. Koryta, *Adv. Colloid and Interface Sci.* **1988**, *29*, 1. c) C. Wei, A. J. Bard, M.V. Mirkin, *J. Phys. Chem. B* **1995**, *99*, 16033. d) J. Zhang, P. R. Unwin, *J. Phys. Chem. B* **2000**, *104*, 2341.
[24] Y. Cheng, D. J. Schiffrin, *J. Chem. Soc. Faraday Trans.* **1996**, *92*, 3865.
[25] C. N. R. Rao, G. U. Kulkarni, P. John Thomas, V. Verun Agrawal, P. Saravanan, *J. Phys. Chem. B* **2003**, *107*, 7391.
[26] F. Reincke, S. G. Hickey, W. K. Kegel, D. Vanmaekelbergh, *Angew. Chem.* **2004**, *116*, 464; *Angew. Chem. Int. Ed.* **2004**, *43*, 458
[27] B. Su, J. P. Abid, D. J. Fermín, H. H. Girault, H. Hoffmannova, P. Kritl, Z. Samec, *J. Am. Chem. Soc.* **2004**, *126*, 915.
[28] M. Platt, R. A. W. Dryfe, E. P. L. Roberts, *Electrochim. Acta* **2003**, *48*, 3037.
[29] R. A. W. Dryfe, A. O. Simm, B. Kralj, *J. Am. Chem. Soc.* **2003**, *125*, 13014.
[30] E. C. Walter, F. Favier, R. M. Penner, *Anal. Chem.* **2002**, *74*, 1546.
[31] a) H. H. Girault, *Electrochimie Physique et Analytique*, Presses Polytechniques et Universitaires Romandes, Lausanne, **2001**, Appendix B. b) T. Heumann, N. D. Stolica in *Encylopaedia of Electrochemistry of the Elements*, *Vol.* V (Ed. A. J. Bard), Marcel Dekker, New York, **1976**, p 137. c) G. M. Schmid, M. E. Curley-Fiorino in *Encylopaedia of Electrochemistry of the Elements*, *Vol.* IV (Ed. A. J. Bard) Marcel Dekker, New York, **1975**, p 94.
[32] N. Eugster, D. J. Fermín, H. H. Girault, *J. Phys. Chem. B* **2002**, *106*, 3428.
[33] H. F. Waibel, M. Kleinert, L. A. Kibler, D. M. Kolb, *Electrochim. Acta* **2002**, *47*, 1461.
[34] M. Platt, R. A. W. Dryfe, E. P. L. Roberts, *Electrochim. Acta* **2004**, *49*, 3937.
[35] T. W. Odom, J. C. Love, D. B. Wolfe, K. E. Paul, G. M. Whitesides, *Langmuir* **2002**, *18*, 5314.
[36] J. H. Lim, C. A. Mirkin, *Adv. Mater.* **2002**, *14*, 1474.
[37] T. Felgenhauer, C. Yan, W. Geyer, H. T. Rong, A. Golzhauser, M. Buck, *Appl. Phys. Lett.* **2001**, *79*, 3323.

Received: June 24, 2004

Early View Article
Published online on November 18, 2004

